Journal of Alloys and Compounds 512 (2012) 33–38

Contents lists available at SciVerse ScienceDirect

Journal of Alloys and Compounds

journal homepage: www.elsevier.com/locate/jallcom

Hydrogen storage properties of cold rolled magnesium hydrides with oxides catalysts

J. Bellemare, J. Huot*

Institut de Recherche sur l'Hydrogène, Université du Québec à Trois-Rivières, 3351 Boul. des Forges, Trois-Rivières, Québec, Canada, G9A 5H7

ARTICLE INFO

Article history:
Received 27 July 2011
Received in revised form 22 August 2011
Accepted 25 August 2011
Available online 3 September 2011

Keywords:
Magnesium hydride
Cold rolling
Catalyst
Crystallite size
Strain

ABSTRACT

In this work, we compared ball milling and cold rolling as a mean to add transition metal oxides to magnesium hydride. We found that irrespective to the mixing technique the oxides NiO and Nb_2O_5 gave the fastest desorption kinetics. In general, sorption kinetics were slightly slower for cold rolled samples compared to their ball milled counterparts. Ball milling 30 min is more effective to get a nanocrystalline structure than rolling 5 times. However, as rolling was performed in air for a limited number of times, it could be expected that rolling under inert atmosphere for a larger number of times will be as effective as ball milling to produce nanocrystalline structure and enhance hydrogen storage properties.

1. Introduction

Because of its high hydrogen storage capacity (7.6 mass%) magnesium hydride (MgH_2) is considered to be a promising hydrogen storage materials. However, the high formation enthalpy changes of MgH_2 (74 kJ/mol H_2) means that it is a relatively stable hydride and makes the rate of hydrogen desorption slow under moderate conditions. It has been shown that increasing sorption kinetics could be obtained by decreasing the crystallite size of magnesium and by using catalysts [1].

Reduction of crystallite size has been achieved mainly by using ball milling method [2–5]. However, scaling-up this type of ball milling to industrial level may be too costly in term of capital and operation cost. Recently, it was shown that cold rolling could achieve the same reduction of crystallite size as ball milling but with an important reduction of processing time and energy [6,7].

Ball milling has also been extensively used to add catalysts to magnesium. A wide range of catalysts has been investigated but a particularly interesting class has been the transition metal oxides [1,8–11]. Amongst the metal oxides studied up to now, Nb_2O_5 seems to be the one giving the faster kinetics [12–23]. Nanosized oxides have also been investigated [24–28]. Recently, some understanding of the catalytic effect of oxide on hydrogen desorption of MgH_2 have been achieved by using the atomization energy concept [29].

As cold rolling has been shown to be much less time consuming than ball milling to produce a nanocrystalline structure [7], we wanted to test the ability of cold rolling to add metal oxides catalysts to magnesium hydride. In this paper we report the use of cold rolling to add oxides of transition metals as catalysts for magnesium hydride. The compounds investigated were MgH_2 + 2 at.%OX, where OX = Co_3O_4, Cr_2O_3, Cu_2O, Fe_2O_3, MnO, Nb_2O_5, NiO, TiO_2, and V_2O_5. As a means of comparison, the same compositions were also processed by ball milling in argon.

2. Experimental method

The cold-rolling apparatus used in this study was a Durston DRM 130 modified in such a way that vertical milling is possible. This configuration enables the processing of powder samples. As starting material we used 300 mesh (50 μm) MgH_2 powder (98% purity) from Alfa Aesar. This MgH_2 was hand mixed with 2 at.% of oxide. The list of oxides studied is presented in Table 1. The oxide Nb_2O_5 is a special case because the compound we used was in fact a mixture of metastable and stable oxides. The composition as determined from Rietveld refinement of the X-ray diffraction pattern of as-received compound is presented in Table 2.

Prior to cold rolling the mixtures were put inside a crucible without any balls and mechanically shaken on a Spex 8000 for 2 min. This procedure ensured a good homogeneity of the mixture without inducing any defects or reduction of crystallite size because no balls were inside the crucible. After mixing, the mixtures were cold rolled in air. Rolling was performed on a Durston DRM 100 modified by the company to have the sample go in vertically. The processing speed was 11 cm/min. After the first roll the powder consolidated in small plates. These plates were cut in two and the two halves superposed for the next roll thus giving a thickness reduction of 50%. However, as the material is in the powder form this reduction should not be taken too literary as there is always some loose powder present. To prevent contamination from the rolls the powder was inserted between two 316 stainless steel plates. After each rolling pass, the mixture was collected and rolled again up to 5 times. Cold rolled materials were kept in air and all handling was done in air.

* Corresponding author. Fax: +1 819 376 5164.
E-mail address: jacques.huot@uqtr.ca (J. Huot).

0925-8388/$ – see front matter © 2011 Elsevier B.V. All rights reserved.
doi:10.1016/j.jallcom.2011.08.085

Table 1
Purity and powder size of catalysts studied. All compounds are from Alfa Aesar. Powder sizes were determined from the mesh size specified by the manufacturer.

	Co_3O_4	Cr_2O_3	Cu_2O	Fe_2O_3	MnO	Nb_2O_5	NiO	TiO_2	V_2O_5
Purity (%)	99.7	99	99	99	99	99.5	99	99	99.6
Powder size ((m)	37	44	74	44	74	149	44	44	1000

Table 2
Composition of as-received Nb_2O_5 as determined from Rietveld refinement of X-ray diffraction pattern. Uncertainty on abundance is ±1 wt.%.

Formula	Nb_2O_5	$Nb_{8.4}O_{21}$	$Nb_{11}O_{27}$	Nb_2O_5	$Nb_{12}O_{29}$
Space group	*I*4/*mmm*	*Pbam*	*P*12/*m*1	*P*12/*m*1	*Cmcm*
Abundance (wt.%)	36	33	16	10	4

In a separate experiment, the same compositions were milled on a Spex 8000 high energy mill in a hardened steel crucible with a powder to ball ratio of 1/10 under argon atmosphere. Milled materials were loaded and removed from the crucible in the protective atmosphere of an argon filled glove box.

The hydrogen sorption properties were measured with a Sieverts-type apparatus. All measurements were performed at 623 K with a hydrogen pressure of 2000 kPa for absorption and 35 kPa (final pressure) for desorption. Sample mass used was about 150 mg and measurements were done on as-rolled powders without any treatment or cycling. The reported curves are thus in fact the first cycle. Crystal structure was analyzed from X-ray powder diffraction patterns registered on a Bruker D8 Focus apparatus with CuKα radiation. Phases abundances as well as crystallite size and microstrain were evaluated from Rietveld method using Topas software [30] via the fundamental parameters approach [31].

3. Results

3.1. Hydrogen sorption properties

First, we will present the effect of transition metal oxides on sorption kinetics of magnesium hydride when the compounds are ball milled 30 min in argon. This will serve as a bench mark for the case when the compounds are cold rolled in air.

3.1.1. Ball milled compounds

The hydrogenation kinetics at 623 K for mixtures of MgH_2 + 2 at.%OX (OX = Co_3O_4, Cr_2O_3, Cu_2O, Fe_2O_3, MnO, Nb_2O_5, NiO, TiO_2, and V_2O_5) ball milled 30 min are shown in Fig. 1. For clarity of the presentation, two separated figures are used to report all results. The amount desorbed is expressed as a ratio of measured capacity over maximum theoretical capacity for each compound. Weight of catalyst was taken into account in evaluation of theoretical capacity. We see that addition of catalyst do not drastically change the hydrogenation kinetics. This is most probably due to the measurement conditions: at 623 K the applied pressure of 20 bar is probably too high compare to the plateau pressure of 6.4 bar. The driving force is too high and it makes comparison between the different catalysts difficult. Nevertheless, some general conclusions could be made. It seems that the oxides Co_3O_4 and Cu_2O have a detrimental effect on the kinetics and reduce the hydrogen capacity. All other catalysts only marginally improve the hydrogenation kinetics. Still, we see that Nb_2O_5 and NiO are the best catalysts. In the case of Nb_2O_5 it has already be identified by other groups as one of the best catalysts for magnesium hydride [12–15].

Dehydrogenation kinetics at 623 K are shown in Fig. 2. Here, there is a clear catalytic effect for all oxides. From the slowest to fastest kinetic the sequence is: Cu_2O, Cr_2O_3, MnO, Co_3O_4, TiO_2, Fe_2O_3, NiO, Nb_2O_5, and V_2O_5. From the dehydrogenation curves we could separate the catalysts in three groups. The first group is made of Cu_2O, Cr_2O_3, and MnO. The faster kinetics of this group is mainly due to the absence of incubation period. A close inspection of the curve of non-catalyzed magnesium shows that from 0 to 300 s the dehydrogenation is very slow and thereafter the rate increases.

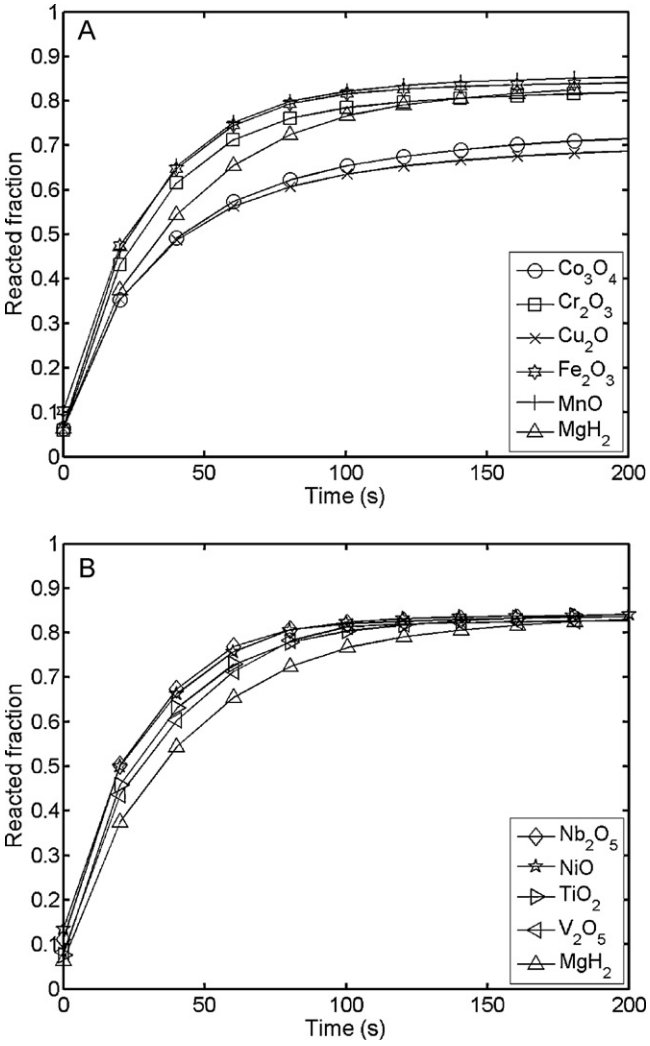

Fig. 1. Hydrogen absorption kinetics at 623 K under 2000 kPa of hydrogen of MgH_2 + 2 at.%OX ball milled 30 min under argon. Capacities are expressed as fraction of theoretical maximum capacity (7.6 wt.%). Weight of the catalyst was subtracted for the calculation of capacities. (A); OX = Co_3O_4, Cr_2O_3, Cu_2O, Fe_2O_5, and MnO: (B); OX = Nb_2O_5, NiO, TiO_2, V_2O_5, and pure MgH_2.

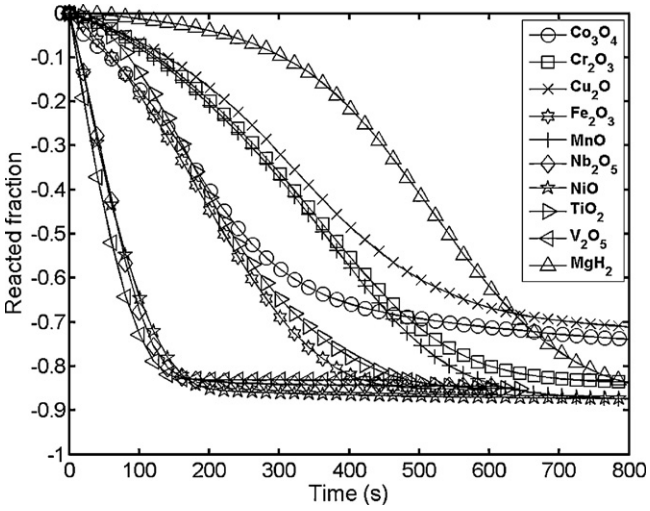

Fig. 2. Hydrogen desorption kinetics at 623 K under 35 kPa of hydrogen of MgH_2 + 2 at.%OX ball milled 30 min under argon. Capacities are expressed as fraction of theoretical maximum capacity (7.6 wt.%). Weight of the catalyst was subtracted for the calculation of capacities.

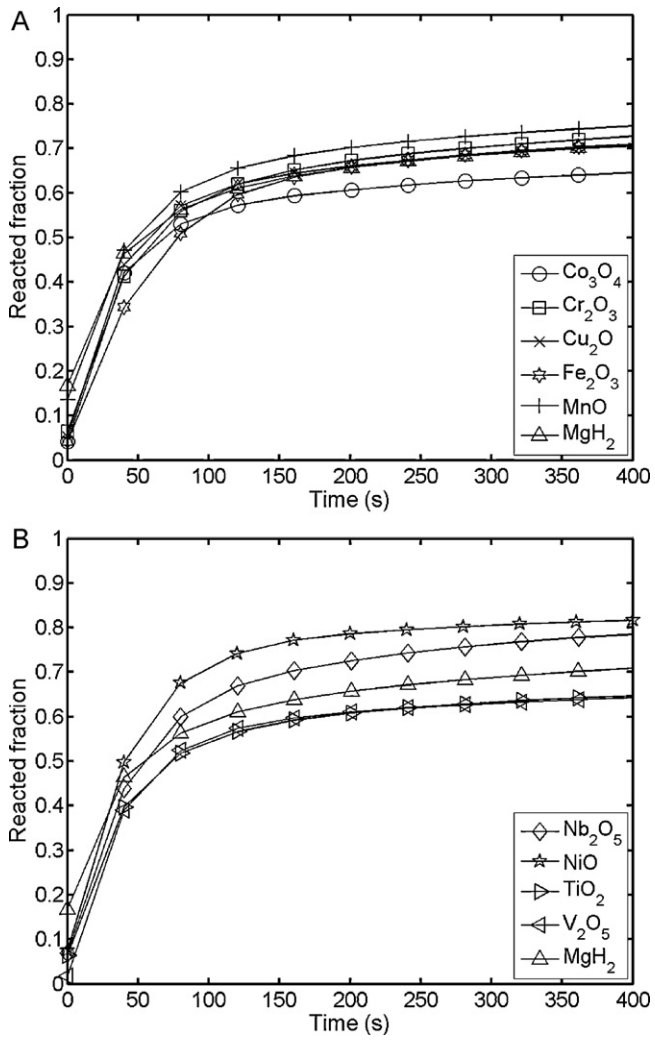

Fig. 3. Hydrogen absorption kinetics at 623 K under 2000 kPa of hydrogen of MgH_2 + 2 at.%OX cold rolled 5 times in air. Capacities are expressed as fraction of theoretical maximum capacity (7.6 wt.%). Weight of the catalyst was subtracted for the calculation of capacities. (A); OX = Co_3O_4, Cr_2O_3, Cu_2O, Fe_2O_5, and MnO: (B); OX = Nb_2O_5, NiO, TiO_2, V_2O_5, and pure MgH_2.

When magnesium hydride is catalyzed with Cu_2O, Cr_2O_3, and MnO there is practically no incubation time and the compounds readily desorb from time zero. However, we see that at mid reaction (near reacted fraction of −0.5) the slope of the curve is bigger for non-catalyzed magnesium than for magnesium catalyzed with Cu_2O, Cr_2O_3, and MnO. Therefore, one may conclude that for these three oxides their effect on magnesium hydride is to almost eliminate the incubation time but also to reduce the intrinsic dehydrogenation kinetics.

The second group of catalysts is made of Co_3O_4, TiO_2, and Fe_2O_3. For these catalysts we see that the incubation time is practically zero and, contrary to the first group, the intrinsic kinetic is as fast as pure magnesium. The dehydrogenation curves are very similar for these three catalyst with the exception of Co_3O_4 which shows a much smaller capacity (about 0.71 reacted fraction) than the two other catalyzed compound. The reason for this decrease is not clear.

Finally, the third group which comprises NiO, Nb_2O_5, and V_2O_5 shows the fastest dehydrogenation kinetics. Here, the incubation time is zero and the intrinsic kinetic is much faster than pure magnesium hydride. After only 200 s the compounds are totally desorbed.

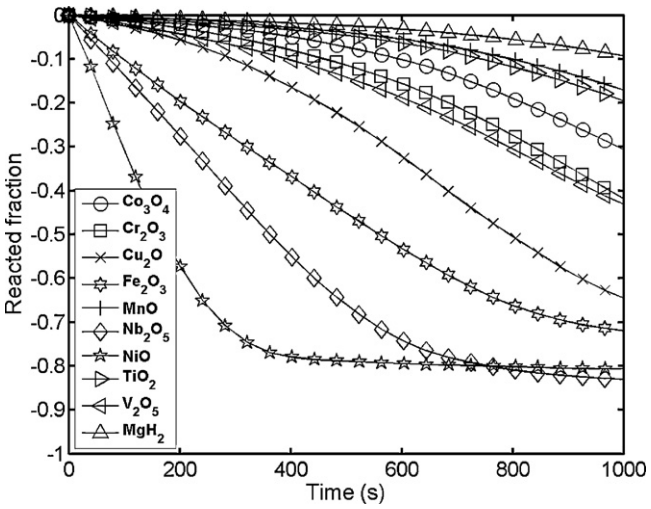

Fig. 4. Hydrogen desorption kinetics at 623 K under 35 kPa of hydrogen of MgH_2 + 2 at.%OX cold rolled 5 times in air. Capacities are expressed as fraction of theoretical maximum capacity (7.6 wt.%). Weight of the catalyst was subtracted for the calculation of capacities.

3.1.2. Cold rolled compounds

Fig. 3 shows the hydrogenation kinetics at 623 K for mixtures of MgH_2 + 2 at.%OX (OX = Co_3O_4, Cr_2O_3, Cu_2O, Fe_2O_3, MnO, Nb_2O_5, NiO, TiO_2, and V_2O_5) cold rolled in air 5 times. Contrary to the ball milled case there is some discrepancies between various catalysts. Kinetics and hydrogen capacities are improved by using NiO and Nb_2O_5 catalysts as in the ball milled case. However, by comparing Fig. 3 with Fig. 1 one can see that the cold rolled samples have a slower kinetic and reduced capacities compared to the same compound ball milled.

Fig. 4 presents the dehydrogenation kinetics at 623 K of cold rolled samples. All oxides have some catalytic effect. From the slowest to fastest kinetic the sequence is: MnO, TiO_2, Co_3O_4, Cr_2O_3, V_2O_5, Cu_2O, Fe_2O_3, Nb_2O_5, and NiO. This sequence is not identical but quite similar to the one presented by ball milled compounds. The rank of most catalyst do not change by more than 3 positions except for Cu_2O, which rank 6 in the cold rolled list but first (slowest compound) in the ball milled list. More important discrepancy is seen for V_2O_5 which is the fastest (rank 10) in the milled list but only 5 for cold rolled. The most probable reason for this discrepancy could be found by inspection of Table 1. We see that the particle size of V_2O_5 is much bigger than the other oxides. For ball milling process this does not make a big difference in term of mixing oxide and MgH_2 because the process last 30 min and good homogeneity is assured. For cold rolling the situation is different because in the first roll the two components are mixed by hand before rolling. As the particles sizes of V_2O_5 and MgH_2 are quite different, mixing is not so homogeneous and moreover during rolling there is surely a segregation of particles. Therefore, just rolling 5 times is not sufficient for good mixing when the two powders have different particle sizes. Thus, the present cold rolling is not as effective as ball milling for inclusion of a catalyst on magnesium hydride. Therefore, the interaction of catalyst and metal hydride is not perfect and the end result depends on the intrinsic nature of the catalyst as well as the preparation method. For some catalyst cold rolling 5 times may be enough to get the full catalytic effect but for other it may not be enough. This is why there is discrepancies between cold rolled and ball milled lists. We expect that if we could find an optimum set of rolling parameters then the cold rolled and ball milled lists will probably be identical or at least more similar than now.

Table 3
Crystallite size and microstrain of the (-MgH_2 phase and phases abundances in wt.% as evaluated from Rietveld refinement of compounds ball milled 30 min in argon. For crystallite size and microstrain values in parenthesis are uncertainties on the last significant digit. For phases abundances error on all values is ±1. For some samples total do not add to 100 because of round-off. Values in square bracket are nominal weight percentage of the catalyst. For Nb_2O_5 M means the metastable phase with space group *I*4/*mmm* and HPHT means the High pressure-High Temperature phase $Nb_{8.4}O_{21}$ with space group *Pbam*.

Catalyst	Abundance (wt.%)				β-MgH_2			Catalyst size (nm)
	β-MgH_2	γ-MgH_2	Mg	MgO	Catalyst	Size (nm)	Microstrain (%)	
–	77	9	3	10	–	16.5(5)	0.88(4)	–
Co_3O_4	63	8	4	7	18 [16]	19.4(7)	0.97(6)	92(4)
Cr_2O_3	68	8	3	9	11 [11]	17.6(4)	0.86(5)	147(9)
Cu_2O	71	7	4	8	8 + $2Cu_{97}Mg_3$ [11]	17.2(3)	0.89(4)	15(1)
Fe_2O_3	68	7	3	12	9 [11]	17.5(4)	0.64(6)	59(4)
MnO	73	9	4	9	5 [5]	17.4(3)	0.87(4)	34(2)
Nb_2O_5	70	7	3	5	M 9 HPHT 6 [17]	16.6(4)	0.71(5)	M 19(1) HPHT 89(6)
NiO	76	8	4	9	6 [6]	16.9(3)	0.80(4)	41(2)
TiO_2	73	8	3	9	7 [6]	16.7(4)	0.95(4)	42(4)
V_2O_5	71	7	4	12	6 [12]	18.4(3)	0.75(3)	17(1)

Table 4
Crystallite size and microstrain of the (-MgH_2 phase and phases abundances in wt.% as evaluated from Rietveld refinement of compounds cold rolled 5 times in air. For crystallite size and microstrain values in parenthesis are uncertainties on the last significant digit. For phases abundances error on all values is ±1. For some samples total do not add to 100 because of round-off. Values in square bracket are nominal weight percentage of the catalyst. For Nb_2O_5 M means the metastable phase with space group *I*4/*mmm* and HPHT means the High pressure-High Temperature phase $Nb_{8.4}O_{21}$ with space group *Pbam*.

Catalyst	Abundance (wt.%)				β-MgH_2			Catalyst size (nm)
	β-MgH_2	γ-MgH_2	Mg	MgO	Catalyst	Size (nm)	Microstrain (%)	
–	82	4	3	7	–	26.1(5)	0.51(3)	–
Co_3O_4	69	4	3	10	13 [16]	30.9(9)	0.33(5)	113(9)
Cr_2O_3	77	2	3	9	9 [11]	33.0(8)	0.66(2)	231(25)
Cu_2O	76	3	4	8	9 [10]	41.3(7)	0.49(2)	19.0(6)
Fe_2O_3	73	5	3	8	10 [11]	23.5(7)	0.39(7)	66(6)
MnO	82	5	3	9	Trace [5]	21.0(5)	0.57(5)	–
Nb_2O_5	78	3	3	3	M 8HPHT 5 [17]	30.2(5)	0.34(3)	M 21(1)HPHT 119(7)
NiO	77	5	3	12	4 [6]	25.2(6)	0.32(5)	57(10)
TiO_2	82	3	3	5	7 [6]	26.8(4)	0.53(2)	35(3)
V_2O_5	82	3	4	3	8 [12]	32.1(4)	0.45(2)	40(2)

3.2. Crystal structure

The crystal structure of all cold rolled and ball milled compounds were analyzed by Rietveld refinement of X-ray powder diffraction patterns. For the present discussion, the most important parameters obtained from Rietveld analysis are the identification and abundance of the phases present in each pattern, the crystallite size and microstrain of β-MgH_2 phase, and the crystallite size of the catalyst. The values of these parameters are reported in Table 3 for the ball milled samples and Table 4 for the cold rolled samples. As representatives, we discuss in more details the three compositions that have the best dehydrogenation kinetics, i.e. MgH_2 doped with NiO, Nb_2O_5, and V_2O_5. For each composition ball milled and cold rolled samples are presented and compared. The powder diffraction pattern of as-received MgH_2 is shown in Fig. 5. The peaks are very sharp, indicating a polycrystalline structure with only MgH_2 and a small amount of Mg presents. A Rietveld refinement gave an abundance of MgH_2 and Mg of respectively 97 wt.% and 3 wt.%. The crystallite size of MgH_2 was 185 nm.

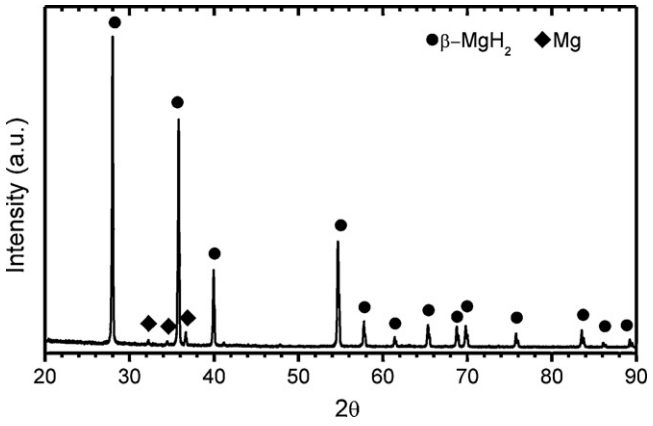

Fig. 5. X-Ray diffraction patterns of as received MgH_2.

Fig. 6 shows the X-ray patterns for MgH_2 doped with NiO. It is clear that both pattern exhibit the same phases but in different abundance. This is confirmed by the Rietveld analysis reported in Tables 3 and 4. We see that the abundances of β-MgH_2, Mg, and NiO phases are essentially the same for cold rolled and ball milled samples. The only difference is in the abundance of the metastable phase γ-MgH_2 and MgO phases. In the case of γ-MgH_2 metastable phase the higher abundance in the ball milled sample could be understood from the higher energy delivered by milling 30 min compared to rolling five times. The higher abundance of MgO phase in the cold rolled sample is also easily explained by the fact that rolling was performed in air while milling was done in argon. Inspection of the diffraction patterns indicates that for the ball milled samples the peaks are broader, especially for higher angles. As the change of peak broadness with angle depends on the microstrain we could expect that the ball milled sample is more highly strained than its cold rolled counterpart. This is confirmed by Rietveld refinement which gave a value of crystallite size for the β-MgH_2 phase of respectively 16.9 nm and 25.2 nm for the ball milled and cold rolled samples while their strain was 0.80% and 0.32%. The crystallite size of NiO is also slightly smaller for the ball milled sample (41 nm) compared to the cold rolled sample (57 nm). All these confirm that ball milling 30 min is slightly more energetic than cold rolling five times. However, more subtle discrepancies could be seen. The relative intensities of the β-MgH_2 and Mg phases in the diffraction pattern of the ball milled sample are in agreement with the references patterns. On the other hand, in the pattern of

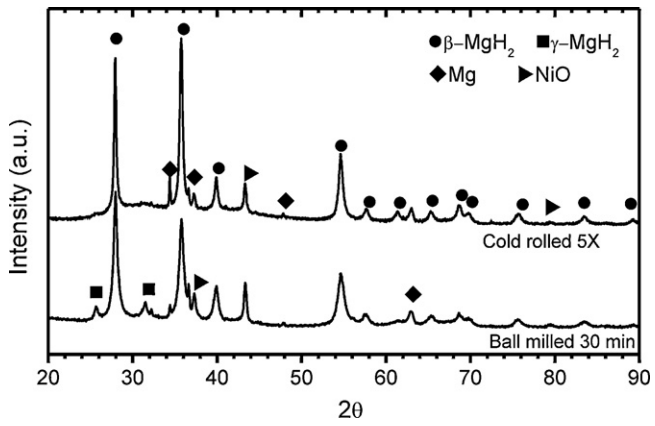

Fig. 6. X-Ray diffraction patterns of MgH_2 + 2 at.%NiO after ball milling 30 min and after cold rolling 5 times.

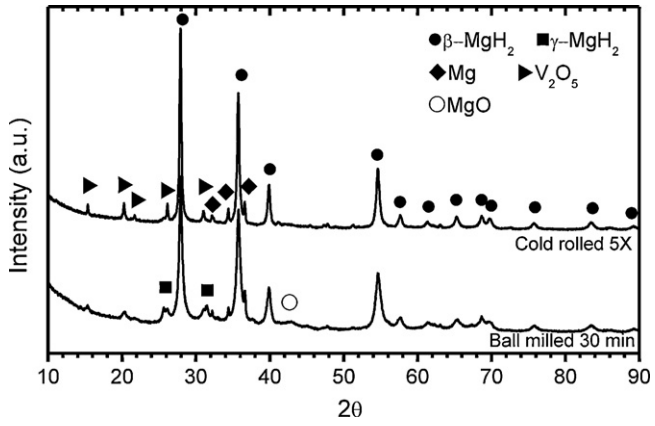

Fig. 7. X-Ray diffraction patterns of MgH_2 + 2 at.%V_2O_5 after ball milling 30 min and after cold rolling 5 times.

the cold rolled sample we see that the relative intensities are not the same. This is an indication that cold rolling induces a texture in the material for both β-MgH_2 and Mg phase. After rolling, the sample is in the form of small plate or flakes. During preparation of the sample for X-ray diffraction these flakes will be preferentially deposited on their flat side on the sample holder which give the preferred orientation seen in the diffraction pattern.

Fig. 7 shows the X-ray diffraction patterns of cold rolled and ball milled MgH_2 doped with V_2O_5. As for the previous case, the crystallite size of β-MgH_2 phase is smaller for the ball milled sample (18 nm) than for the cold rolled sample (32 nm) while the microstrain is higher in the ball milled sample (0.75%) than for the cold rolled sample (0.45%). Also, as in the NiO case the crystallite size of V_2O_5 is bigger in the cold rolled sample (40 nm) than in the ball milled one (17 nm). One interesting observation is the high abundance of MgO in the ball milled sample. Actually, even if milling was performed in argon and rolling in air the abundance of MgO is higher in the ball milled sample. A possible explanation could be put forward by examining the phase abundance of V_2O_5. We see that in the ball milled sample the abundance is only 6 wt.% which is almost one half of the nominal content. We thus explain the appearance of MgO by the fact that milling is so intense that some of MgH_2 will react with V_2O_5. Magnesium being more easily oxidized than vanadium there may be transfer of oxygen from vanadium to magnesium. Because the abundance of magnesium is the same as in the starting powder (4 wt.%) and the β-MgH_2 phase is depleted (71 wt.%) we conclude that it is the magnesium hydride phase that is reacting with vanadium oxide to produce magnesium oxide. The

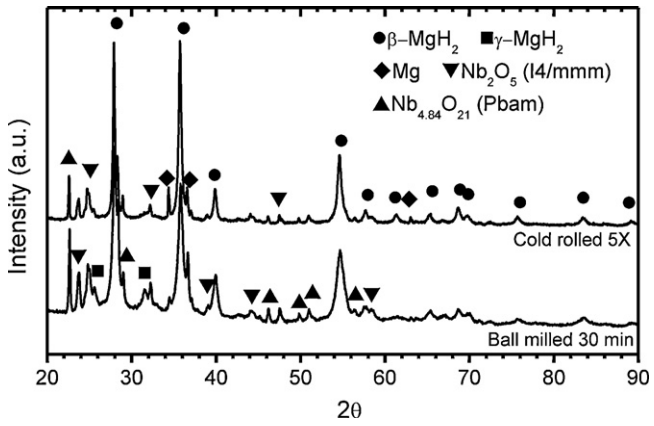

Fig. 8. X-Ray diffraction patterns of MgH_2 + 2 at.%Nb_2O_5 after ball milling 30 min and after cold rolling 5 times.

pure vanadium peaks are not seen because the main Bragg peaks of vanadium are almost at the same angle as the MgO peaks. As we expect that the crystallite size of vanadium will also be very small these peaks are essentially buried into the background and are practically impossible to identify. Finally, it should be pointed out that here the pattern of the cold rolled sample does not show any texture. This may be an indication that the transition metal oxide has also some mechanical effect on the effectiveness of rolling.

The diffraction patterns of ball milled and cold rolled MgH_2 doped with Nb_2O_5 are shown in Fig. 8. As for the two previous cases, for β-MgH_2 phase, ball milling produces smaller crystallite size (17 nm) and higher microstrain (0.7%) than cold rolling (respectively 30 nm and 0.3%). Due to the multiphase nature of Nb_2O_5, only the two principal phases could be indentified in the MgH_2 + Nb_2O_5 mixture: Nb_2O_5 (*I*4/*mmm*) and $Nb_{8.4}O_{21}$ (*Pbam*). The pattern of cold rolled sample shows a slight texture for both β-MgH_2 and Mg phase.

Inspection of Tables 3 and 4 shows that the crystallite size and microstrain of β-MgH_2 are essentially the same for all ball milled compounds. In the case of cold rolled compounds, the variation of these parameters is greater but globally we see that crystallites sizes are bigger than their ball milled counterparts and microstrain smaller. This is a good indication that cold rolling five times is not as effective to produce nanocrystalline materials as ball milling 30 min. The same situation is seen for the crystallite size of the oxide: ball milling produces smaller crystallite size than cold rolling.

Some peculiar features were seen in two systems. First, for MgH_2 doped with MnO although the nominal abundance of MnO was found in the X-ray pattern of ball milled compound only a trace was seen in the cold rolled sample pattern. The exact reason for this behaviour is not clear but as this oxide do not drastically enhance hydrogen sorption even for ball milled material we did not investigate this matter further. Second, for MgH_2 doped with Cu_2O and ball milled the X-ray pattern showed the formation of the alloy $Cu_{97}Mg_3$ with an abundance of 2 wt.%. This alloy was not formed by cold rolling thus giving another indication of the higher energy of milling compared to cold rolling.

4. Conclusion

In this work, magnesium hydride was doped with transition metal oxides by using two different techniques: ball milling and cold rolling. We found that irrespective to the mixing technique the oxides NiO and Nb_2O_5 gave the fastest desorption kinetics. In the case of V_2O_5 it is well known to be a good catalyst and it was confirmed in our ball milled sample. However, the

corresponding cold rolled sample showed relatively slow desorption kinetics. This could be explained by the fact that particle size of V_2O_5 was much bigger than particle size of MgH_2 and the mixing of these two was incomplete. This gives a fundamental difference between ball milling and cold rolling: mixing is much more difficult in the later case and five rolling passes as in the present study are not sufficient for complete mixing.

We also found that ball milling 30 min is more effective than five rolling passes to get a nanocrystalline structure. However, it should be pointed out that performing five rolling passes takes less than 1 min. Moreover, the rolling was performed in air while milling was done in argon. Therefore, even if the hydrogen sorption performances of cold rolled samples were not as good as the ball milled ones, there is much room for improvement by first performing cold rolling under inert atmosphere and secondly by rolling a much higher number of times. Thus, this preliminary work indicates that there is some potential for cold rolling to be a technique for adding catalysts to metal hydrides.

Acknowledgements

This work was funded by the Natural Sciences and Engineering Research Council of Canada (NSERC). J. Bellemare would like to thanks NSERC for a summer fellowship.

References

[1] G. Barkhordarian, T. Klassen, R. Bormann, Journal of Physical Chemistry B 110 (2006) 11020–11024.
[2] A. Zaluska, L. Zaluski, J.O. Ström-Olsen, Journal of Alloys and Compounds 288 (1999) 217–225.
[3] G. Liang, J. Huot, S. Boily, A.V. Neste, R. Schulz, Journal of Alloys and Compounds 292 (1999) 247–252.
[4] J. Huot, G. Liang, R. Schulz, Applied Physics A 72 (2001) 187–195.
[5] B. Sakintuna, F. Lamari-Darkrim, M. Hirscher, International Journal of Hydrogen Energy 32 (2007) 1121–1140.
[6] D.R. Leiva, J. Huot, T.T. Ishikawa, C. Bolfarini, C.S. Kiminami, A.M. Jorge, W.J. Botta, Materials Science Forum 667–669 (2011) 1047–1051.
[7] J. Lang, J. Huot, Journal of Alloys and Compounds 509 (2011) L18–L22.
[8] W. Oelerich, T. Klassen, R. Bormann, Journal of Alloys and Compounds 315 (2001) 237–242.
[9] M.Y. Song, J.-L. Bobet, B. Darriet, Journal of Alloys and Compounds 340 (2002) 256–262.
[10] K.S. Jung, E.Y. Lee, K.S. Lee, Journal of Alloys and Compounds 421 (2006) 179–184.
[11] M. Polanski, J. Bystrzycki, T. Plocinski, International Journal of Hydrogen Energy 33 (2008) 1859–1867.
[12] N. Hanada, T. Ichikawa, H. Fujii, Journal of Alloys and Compounds 446–447 (2007) 67–71.
[13] N. Hanada, T. Ichikawa, H. Fujii, Journal of Alloys and Compounds 404–406 (2005) 716–719.
[14] G. Barkhordarian, T. Klassen, R. Bormann, Scripta Materialia 49 (2003) 213–217.
[15] G. Barkhordarian, T. Klassen, R. Bormann, Journal of Alloys and Compounds 364 (2004) 242–246.
[16] D. Fátay, Á. Révész, T. Spassov, Journal of Alloys and Compounds 399 (2005) 237–241.
[17] P.A. Huhn, M. Dornheim, T. Klassen, R. Bormann, Journal of Alloys and Compounds 404–406 (2005) 499–502.
[18] K.F. Aguey-Zinsou, J.R. Ares Fernandez, T. Klassen, R. Bormann, International Journal of Hydrogen Energy 32 (2007) 2400–2407.
[19] O. Friedrichs, F. Aguey-Zinsou, J.R.A. Fernandez, J.C. Sanchez-Lopez, A. Justo, T. Klassen, R. Bormann, A. Fernandez, Acta Materialia 54 (2006) 105–110.
[20] O. Friedrichs, T. Klassen, R. Bormann, A. Fernandez, Scripta Materialia 54 (2006) 1293–1297.
[21] O. Friedrichs, J.C. Sanchez-Lopez, C. Lopez-Cartes, T. Klassen, R. Bormann, A. Fernandez, Journal of Applied Chemistry B 110 (2006) 7845–7850.
[22] N. Hanada, E. Hirotoshi, T. Ichikawa, E. Akiba, H. Fujii, Journal of Alloys and Compounds 450 (2008) 395–399.
[23] N. Hanada, T. Ichikawa, S. Hino, H. Fujii, Journal of Alloys and Compounds 420 (2006) 46–49.
[24] J.-L. Bobet, S. Desmoulins-Krawiec, E. Grigorova, F. Cansell, B. Chevalier, Journal of Alloys and Compounds 351 (2003) 217–221.
[25] R.A. Varin, T. Czujko, E.B. Wasmund, Z.S. Wronski, Journal of Alloys and Compounds 446–447 (2007) 63–66.
[26] K.S. Jung, D.H. Kim, E.Y. Lee, K.S. Lee, Catalysis Today 120 (2007) 270–275.
[27] K.-F. Aguey-Zinsou, T. Nicolaisen, J.R.A. Fernandez, T. Klassen, R. Bormann, Journal of Alloys and Compounds 434–435 (2007) 738–742.
[28] M. Polanski, J. Bystrzycki, Journal of Alloys and Compounds 486 (2009) 697–701.
[29] H. Hirate, Y. Saito, I. Nakaya, H. Sawai, Y. Shinzato, H. Yukawa, M. Morinaga, T. Baba, H. Nakai, International Journal of Quantum Chemistry 109 (2009) 2793–2800.
[30] BRUKER_AXS, TOPAS V4. General profile and structure analysis software for powder diffraction data, Karlsruhe, Germany, (2008).
[31] R.W. Cheary, A.A. Coelho, J.P. Cline, Journal of Research of the National Institute of Standard and Technology 109 (2004) 1–25.